

Experimental Investigations on Adding Alumina on Automotive Disc Brake Pads and Effect on Brake Performance

Sayed Saad Mohamed Saleh¹, Ibrahim Ahmed¹, Ahmed A. A. Saad², Yasser Fatouh¹, Khaled Abdelwahed¹

Department of Automotive and Tractor Technology, Faculty of Technology and Education, Helwan University, Helwan, Egypt

Department of Automotive Engineering, Faculty of Engineering, Mataria, Helwan University, Helwan, Egypt
Corresponding Author: Sayed Saad Mohamed Saleh.

Abstract: In a single formulation, automotive brake pads contain multiple components that contribute to a stable and consistent friction coefficient under various operating conditions, such as sliding speed, operating temperatures, and brake oil pressure. This study aims to improve brake performance by adding alumina as an abrasive to disc brake pad formulations in varying proportions. Three experimental formulations were prepared: the first is the conventional formulation of a Honda Excel passenger car disc brake pad without alumina (0 vol%) alumina (A), the second is the modified formulation (B) with (0.5 vol%) alumina, and the third is the modified formulation (C) with (3 vol%) alumina according to the conventional formulation. The results of laboratory experiments indicated that samples (b) and (c) have consistent and stable braking performance under some different operating conditions, and sample (a) has lower operating temperatures than samples (b) and (c), and sample (b) is the best combination according to the results of the other samples.

Keywords: Friction coefficient, Brake pad, Disc brake, Brake oil pressure, Brake performance, Automotive Disc Brake

Date of Submission: 10-05-2025

Date of acceptance: 20-05-2025

I. Introduction

To ensure the safety of passengers first and then vehicles, the car's brake system is an important component to prevent collisions by controlling the car's speed and steering [1-2] (Mr. Ajeet B. Bhane et al., 2020; Fauzan Ilham Maulana et al., 2019). Braking performance is affected by several factors, including sliding speed, brake fluid pressure, friction coefficient, torque, braking force, and brake pad materials (Ibrahim L. Ahmed et al., 2020). For the brake system to perform as required, there must be friction to convert kinetic energy into thermal energy resulting from friction between the pad and the rotor. Therefore, brake pads play an important role in the brake system. According to ASTM standards, brake pads have been developed. Brake pads are made of approximately 17 components, 14 of which are modifiable, while the rest remain virtually constant, (Shoaib Munir Mulani et al., 2022; Matteo Federici et al., 2018). Brake pad composites contain a variety of materials that ensure high resistance, thermal stability, and frictional stability under constantly changing operating conditions. These materials include ferrous and non-ferrous (metallic components), as well as non-metallic components, as well as binders and lubricants, to ensure good and stable performance under difficult friction conditions, some formulations also contain organic fibers, metal oxides, and carbon nanomaterials, including natural fibers such as banana peels and palm kernels, which enhance mechanical and frictional properties. (Ileana Nicoleta et al., 2015; Senthil Kumaran Selvaraj et al., 2021; Zeina Ammaret et al., 2023). Some brake pad composite materials contain a combination of abrasives and lubricants, as well as natural fibers such as palm and flax, along with inorganic materials such as barium sulfate, to improve frictional properties and reduce negative impact on the environment and humans (G. Gautier di Confiengo, 2022). Many studies have been conducted to study various brake pad compounds and find alternatives to traditional materials and their impact on various factors. This study aims to find alternative environmental materials to replace the traditional materials used in brake pad assemblies. Coconut fibers were used to obtain results that help in obtaining excellent frictional properties, (C Pinca-Bretotean et al., 2021). In this research paper, the results of a brake pad formulation containing palm kernel shell, epoxy resin and alumina up to 6% by volume were discussed and it was found that this formulation has good frictional properties (Mastariyanto Perdana et al., 2023). In this study, a brake pad formulation containing SIC and an aluminum matrix was prepared, which was manufactured by traditional casting. This formulation was characterized by good frictional performance and was recommended as an alternative to traditional materials (Arpita Chatterjee et al., 2023). This research paper aimed to develop composite brake pad material consisting of variable proportions of coconut fiber (0%, 5%,

10%, 15%) and alumina matrix. Satisfactory results were obtained, such as thermal stability and stable friction coefficient (A L Crăciun et al., 2017). The composite material in this study contains alumina, coconut fiber, zirconium oxide, titanium, and silicon carbide. Experiments were conducted on different brake pad formulations, and the results demonstrated stable properties and reduced noise and vibration during braking (A L Craciun et al., 2018). The composite material in this study includes various sugarcane fiber compounds at ratios ranging from 5 to 20% by weight. The results demonstrated stable properties and improved wear resistance during friction (Vikas Mehta et al., 2023). This research paper discusses the performance of a composite material containing rice straw ash, alumina and teak wood powder at fixed ratios of 30% for each material and different combinations of other samples. The results showed satisfactory performance of the samples tested (Moch. Aziz Kurniawan et al., 2022). This research paper discusses the performance of composite material containing 52% coconut shell, 8% alumina, and 35% epoxy resins, results showed good performance of the formulations tested (J. Abutu1 et al., 2018). This research paper discusses composite brake pad material containing variable amounts of steel fibers (0-20% by weight), phenolic binder resin, cashew nut shell, and aramid core, with the aim of enhancing the frictional properties and improving wear (J. Abutu1 et al., 2018). This study tested natural zeolite in different brake pad formulations as a ceramic-like material in behavior due to its silica content and compared the results with formulations of samples containing zeolite mixed with normal elements (Ahmet Keskin, 2011). This study used river sand and wheat straw fibers as a binder. Epoxy resin was added to different brake pad formulations. These components were identified and prepared to enhance the vehicle's frictional performance. The results showed good performance of samples tested (Worku MamuyeYilma et al., 2023). To improve the brake pad properties, composites containing aluminum oxides, cellulose fibers, and graphite were used. The results showed that the research samples had stable thermal performance and improved wear rate (Dinesh S Marewad et al., 2018). This study discussed composite brake friction materials with variable ratios consisting of hemp, pineapple, and banana fibers. The results were evaluated according to the following properties: friction coefficient and wear. Laboratory results indicated improved braking performance (Tej Singh et al., 2023). The advanced brake pad composite material contains sawdust, resin, carbon black, copper flakes, zinc oxide, and sulfur. These ingredients are blended and produced together to ensure safety and performance without asbestos (Benedict U. Iyida et al., 2023). By referring to research papers related to this study which aim to provide information and find solutions and alternatives through the development of composite materials for brake pads to reduce environmental pollution and manufacturing costs.

This study aims to obtain different brake pad formulations containing nano-aluminum oxide powder to improve braking performance. During laboratory experiments, frictional, braking force, and braking torque were considered under various operating conditions, such as sliding speed, operating temperature, braking time, and brake oil pressure.

II. Experimental Setup

Raw materials

Laboratory experiments were conducted on a conventional composition for a passenger car, disc brake pad sample (a). It contained silicon 0.11 vol%, iron 70 vol%, phosphorus 0.005 vol%, sulfur 0.01vol%, manganese 0.619 vol%, chromium 0.030 vol%, titanium 0.297 vol%, niobium 0.029 vol%, 10 vol% phenol, 7 vol% graphite, and 11.9 vol% barite by volume and for the other test samples, nano-sized aluminum oxides were added as the main component and abrasive at variable rates to modified sample (B), first at 0.5 vol% by volume, and to modified sample (C), aluminum oxides were added at 3 vol% by volume.

The main components of the test rig

The purpose of the braking performance test rig as shown in Fig. 1, used in this study is to generate the kinetic energy required for conducting the experiments and to overcome it during the braking process by means of a disc brake system and to prepare the appropriate operating conditions for each of the research experiments. The testing device used in the laboratory experiments of this study was designed and assembled in Lab B104, Department of Automotive and Tractor Technology, Faculty of Technology and Education, Helwan University.

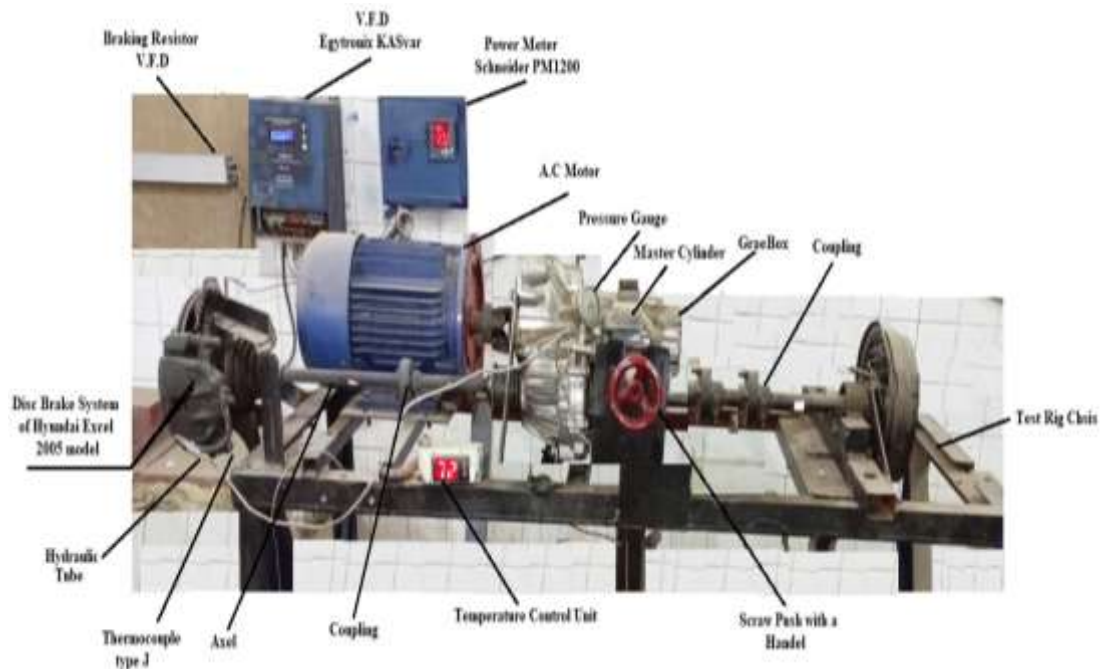


Fig. 1 Main components of the test rig

Disc brake system

Floating-piston disc brake pads from a 2005 Hyundai Excel passenger car were used in the test rig. The brake system used consists of a single-piston caliper, bolts, a brake pad, and a single-piston hydraulic wheel cylinder as shown in Fig 2.



Fig. 2 Disc brake system of hyundai excel 2005 model

Disc brake pad

In Fig 3 shows the disc brake pad used in the brake system of the testing device. There are three samples for testing: Sample (A), which is the conventional sample without alumina; Sample (B), which contains (Al₂O₃- 0.5 vol%) compared to the total volume of the conventional sample; and Sample (C), which contains (Al₂O₃- 3 vol%) compared to the conventional sample.



Fig. 3 Disc brake pad of test rig

The normal force generation unit

The braking force is affected by several factors, including the applied force (F_n), friction coefficient (μ) (Rewida Sami Abdullah et al., 2022), a hydraulic power generation unit has been added to test rig, which supplies the brake unit with friction with the brake disc. Because the brake oil is incompressible, the effect is achieved through the hydraulic unit equipped with a pulley, through which the pressure is applied, which is transferred by the brake oil to be transformed into a frictional force that works to stop the brake disc by friction through the slave cylinder, applied force was calculated using the following equations:

$$A_s = \frac{\pi}{4} D_s^2 \quad (1)$$

$$P = \frac{F_n}{A_s} \quad (2)$$

$$F_n = P * A_s \quad (3)$$

Where:

D_s piston diameter of slave cylinder equals (0.052 m)

A_s piston area of slave cylinder equals ($2.12 \cdot 10^{-3} \text{m}^2$)

F_n Applied force of the disc brake system which affects brake pad, was selected oil pressure values of 5 and 10 bar are selected during the tests. According to Eq. (3), these values of pressure equal applied force of 1103, and 2206 N respectively for disc brake system.

The kinetic energy generation unit

The coefficient of friction is affected by many factors, including the sliding speed, which affects the torque and braking force (Khaled Abdelwahed et al., 2018). In this study, a brake force meter was used using an electric motor with a capacity of up to 7.5 kilowatts and a rotational speed of up to 2900 r.p.m.

Temperature measurement unit

Braking efficiency is affected by temperature (Siti Shofiah et al., 2024), so in this study, a digital temperature measuring unit with a J-type thermocouple with a measuring range of 700°C was designed and prepared to measure the initial operating temperatures at 70, 100, and 130°C and the final operating temperatures during laboratory experiments within 60 seconds.

Speed measurement and brake torque calculation

The braking system is affected by the braking torque, which is measured by a Schneider PM 1200 digital power meter and ranges from 20 to 300 kW. The braking torque is measured by the electric motor, as shown in Fig. 4. To measure the rotational speed of the brake disc, a digital tachometer DT6234 was used, with a range of up to 100,000 rpm, as shown in Fig. 5.



Fig. 4 Schneider PM 1200 digital



Fig. 5 Digital tachometer DT6234B

By measuring the brake power and knowing the angular velocity of the rotating disc, the braking torque can be calculated. Laboratory experiments were conducted at a sliding speed of 300 and 600 rpm, and the braking force was calculated using the following equations:

$$\omega = \frac{2\pi n}{60} \quad (4)$$

$$T_b = \frac{P_b}{\omega} \quad (5)$$

Where:

- n Sliding speed of the rotating disc (r.p.m)
- ω Angular speed of the rotating disc (rad/sec.)
- P_b Brake power (watt)
- T_b Brake torque (N.m)

Brake force and friction coefficient calculations

The brake system is affected by the coefficient of friction and the brake force. In this study, the following equations are used to calculate the coefficient of friction as follows:

$$R_{eff} = \frac{r_i + r_o}{2} \quad (6)$$

Where:

- R_{eff} Effective radius of brake pad, equals 0.089 (m).
- r_i Inner radius of the brake pad (m).
- r_o Outer radius of the brake pad (m).

$$F_b = \frac{T_b}{R_{eff}} \quad (7)$$

$$\mu = \frac{F_b}{F_n} \quad (8)$$

Where:

- F_b Brake force (N).
- μ Friction coefficient.

III. Results And Discussion

The following parameters were investigated during laboratory experiments to evaluate the performance of the brake system for study samples A, B, and C: the initial operating temperature was carried out at 70 and 130°C, sliding speed at 150 and 600 rpm, and the brake oil pressure at 2.5 and 10 bar. The final operating temperature and braking power were measured in each experiment during the braking process for 60 seconds.

Effect of brake oil pressure at sliding speed 150 and 600 r.p.m at initial temperature 70 and 130°C on mean brake force

Fig. 6 shows that the average brake force of commercial and modified samples at temperatures of 70 and 130°C at a constant sliding speed of 150 rpm. The results show that the average brake force of commercial sample (A) at 70°C is 130.91 and 958.24 N, for modified sample (B) are 148.91 and 1084.59 N, and for modified sample (C) are 140 and 1033.46 N and at an initial temperature of 130°C, the average brake force for commercial sample (A) was 125.83 and 948 N, for modified sample (B) 147 and 1074.37 N, and for modified sample (C) 138.35 and 1014.26 N, respectively at brake oil pressure of 2.5 and 10 bar, the value of mean brake force of sample (B) increases by 12.16%, 11.62% and for sample (c) increases by 7.14%, 7.26% depending on value of mean brake force of commercial sample (A).

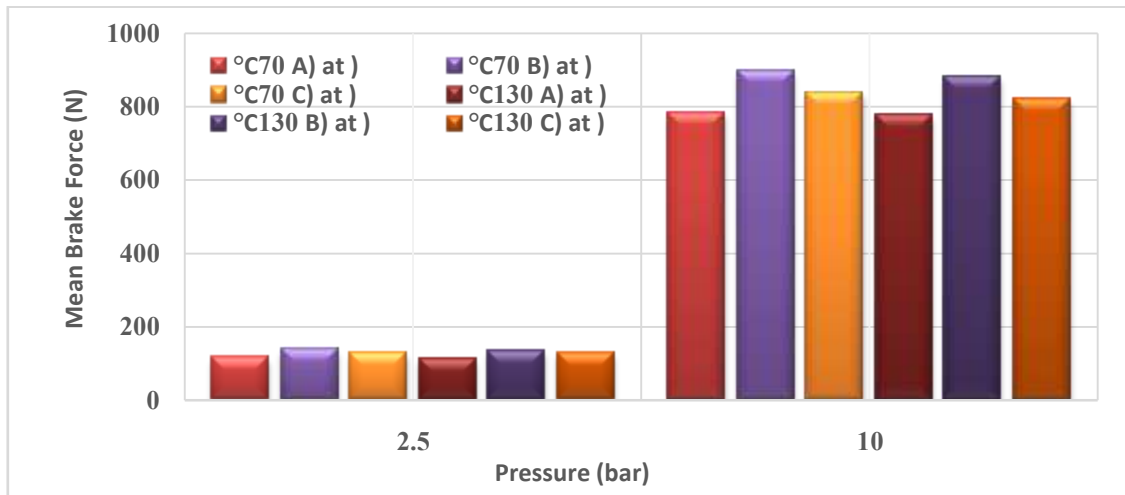


Fig. 6. Effect of pressure on mean brake force of commercial and modified samples at sliding speed 150 r.p.m

In Fig. 7 shows that the average brake force of commercial and modified samples at temperatures of 70 and 130°C at a constant sliding speed of 600 rpm at brake oil pressure 2.5 and 10 bar. The results show that the average brake force of commercial sample (A) at 70°C is 114.50 and 784.6718 N, for modified sample (B) are 136.58 and 895.26 N, and for modified sample (C) are 128.70 and 838.42 N and at an initial temperature of 130°C, the average brake force for commercial sample (A) was 112.59 and 775.52 N, for modified sample (B) 132.74 and 879.80 N, and for modified sample (C) 126.15 and 818.48 N, respectively at brake oil pressure of 2.5 and 10 bar, the value of mean brake force of sample (B) increases by 16.17%, 12.40% and for sample (c) increases by 10%, 6.44% depending on value of mean brake force of commercial sample (A).

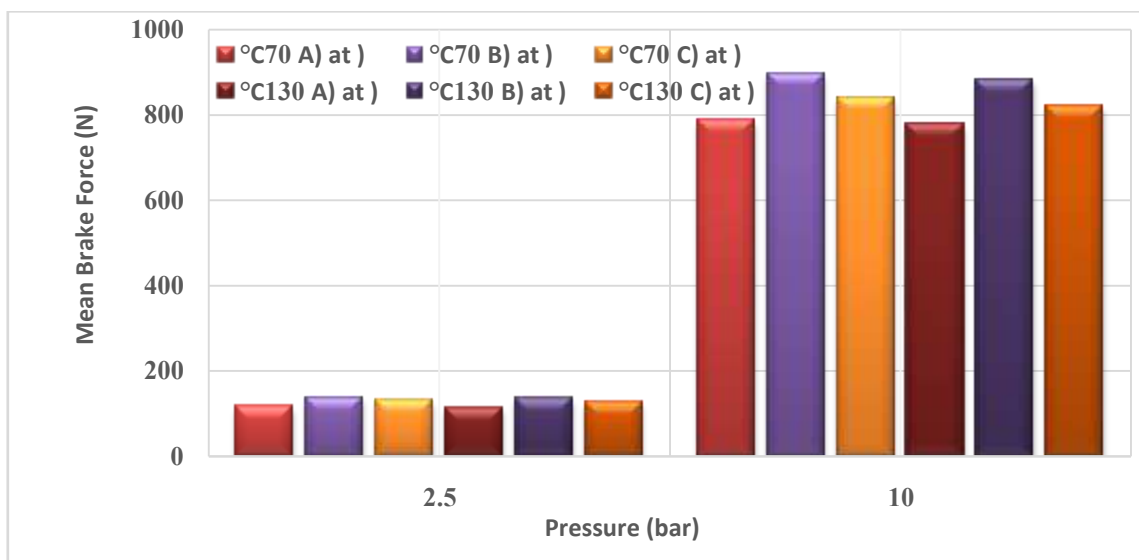


Fig. 7. Effect of brake oil pressure on mean brake force of commercial and modified samples at sliding speed 600 r.p.m

Effect of brake oil pressure on mean friction coefficient of commercial and modified samples at initial temperature 70°C at sliding speed

In Fig. 8 and Fig. 9 shows the effect of brake oil pressure of 2.5 and 10 bar on average friction coefficient at sliding speeds of 150 and 600 rpm and initial operating temperature of 70°C. The average friction coefficients for modified samples (B) and (C) are higher than the average friction coefficients for commercial sample (A), because alumina is an abrasive with nanometer diameters that enhances the coefficient of friction.

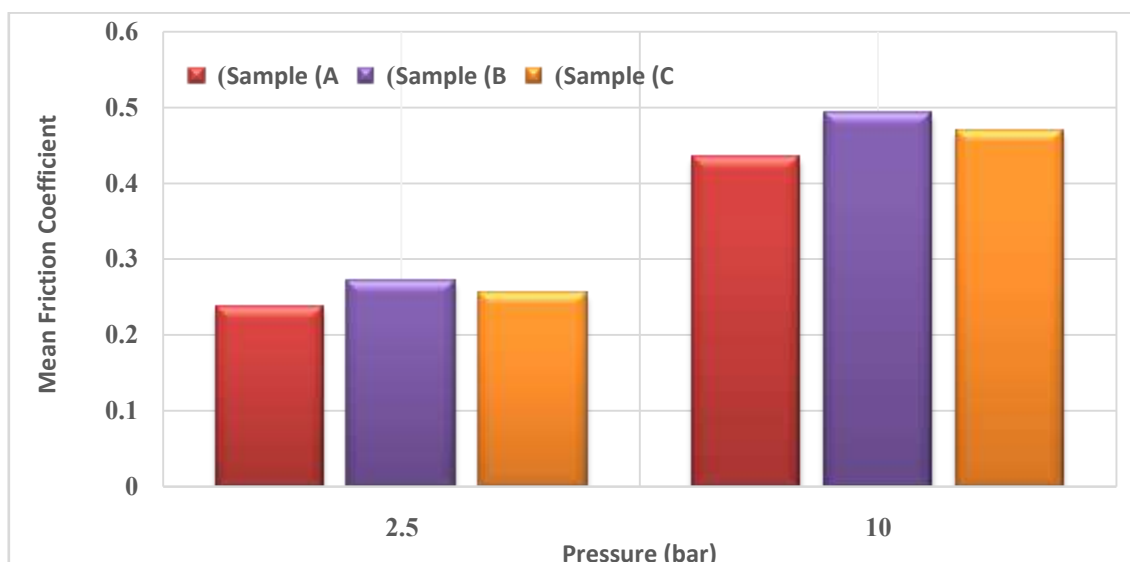


Fig. 8. Effect of brake oil pressure on mean friction coefficient of commercial and modified samples at sliding speed 150 r.p.m and at initial temperature 70°C

By increasing brake oil pressure from 2.5 to 10 bar, the average friction coefficient for the commercial sample (A) increased from 0.237 to 0.434, for the modified sample (B) from 0.270 to 0.491, and for the modified sample (C) from 0.253 to 0.468, also the results shown at sliding speed 600 rpm by increasing brake oil pressure from 2.5 to 10 bar, the average friction coefficient for the commercial sample (A) increased from 0.207 to 0.355, for modified sample (B) from 0.247 to 0.405, and for the modified sample (C) from 0.233 to 0.380. The results show an improvement in average friction coefficients for the modified samples due to the addition of nano-sized alumina and the improvement of the friction surfaces.

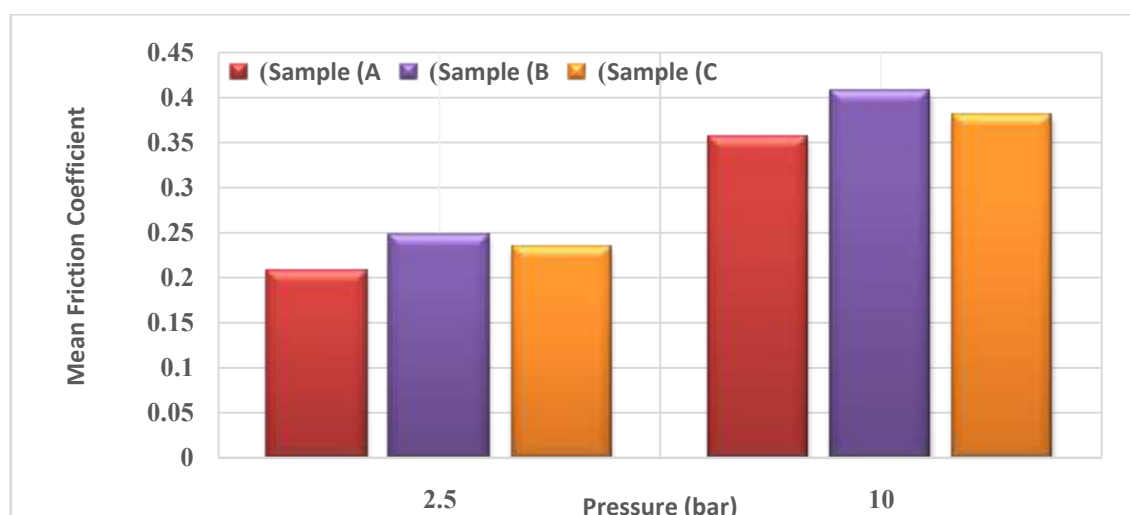


Fig. 9. Effect of brake oil pressure on mean friction coefficient of commercial and modified samples at sliding speed 600 r.p.m and at initial temperature 70°C

Effect of alumina on the operating temperature of commercial and modified brake pads

The effect of alumina on operating temperatures of commercial and modified brake pads at a sliding speed of 600 rpm at initial operating temperatures of 70°C is shown in Fig. 10. The results show a lower final

temperature for commercial sample (A) compared to modified samples (B, C) at 2.5 and 10 bar pressures. This is due to the lower coefficient of friction of commercial sample. The final temperatures for sample (A) are 73 and 95°C, for sample (B) 79 and 104°C, and for sample (C) 75 and 100°C, respectively at brake oil pressures of 2.5 and 10 bar.

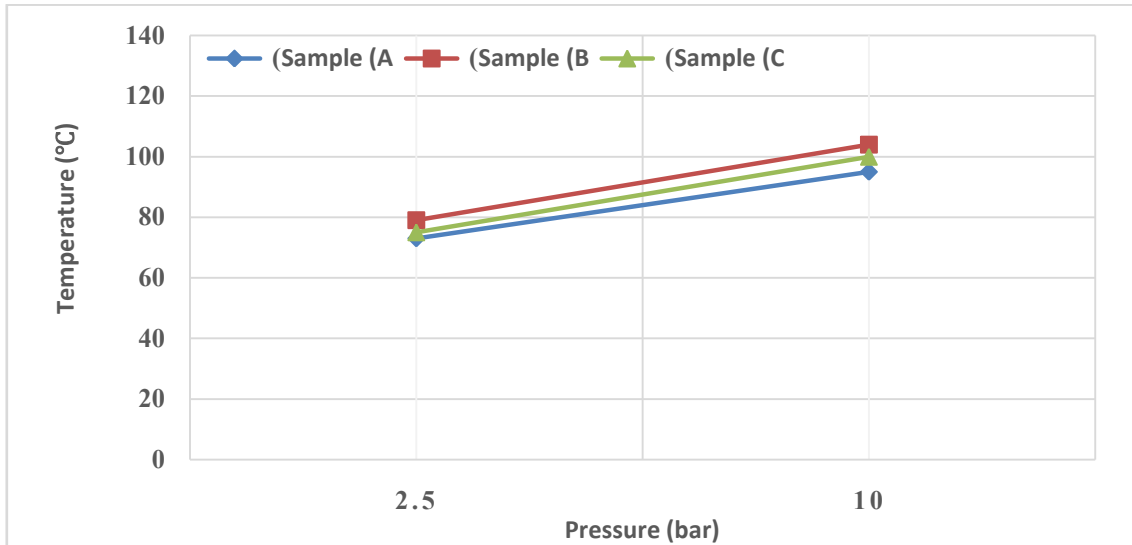


Fig. 10. Effect of alumina on the operating temperature of commercial and modified brake pads at a sliding speed of 600 rpm at initial operating temperatures of 70°C

Effect of alumina on brake tourq of commercial and modified brake pads at sliding speed

At an initial temperature of 70°C, the results on Fig. 11, 12 show the effect of alumina on brake torque of commercial and modified samples at a sliding speed of 600 rpm. The average brake torque for commercial sample (A) is 19.19 and 137.38 N.m, for the modified sample (B) is 25.40 and 156.74 N.m, and for sample (C) is 21.32 and 146.79 N.m at a pressure of 2.5 and 10 bar, respectively. Also, the results showed that the average brake torque of modified samples was higher than the average brake torque of commercial sample with an increase in brake oil pressure from 2.5 to 10 bar and a sliding speed of 600 r.p.m. during a braking time of 60 seconds. This is due to the increase in brake power and friction coefficient under the same operating conditions at each constant speed.

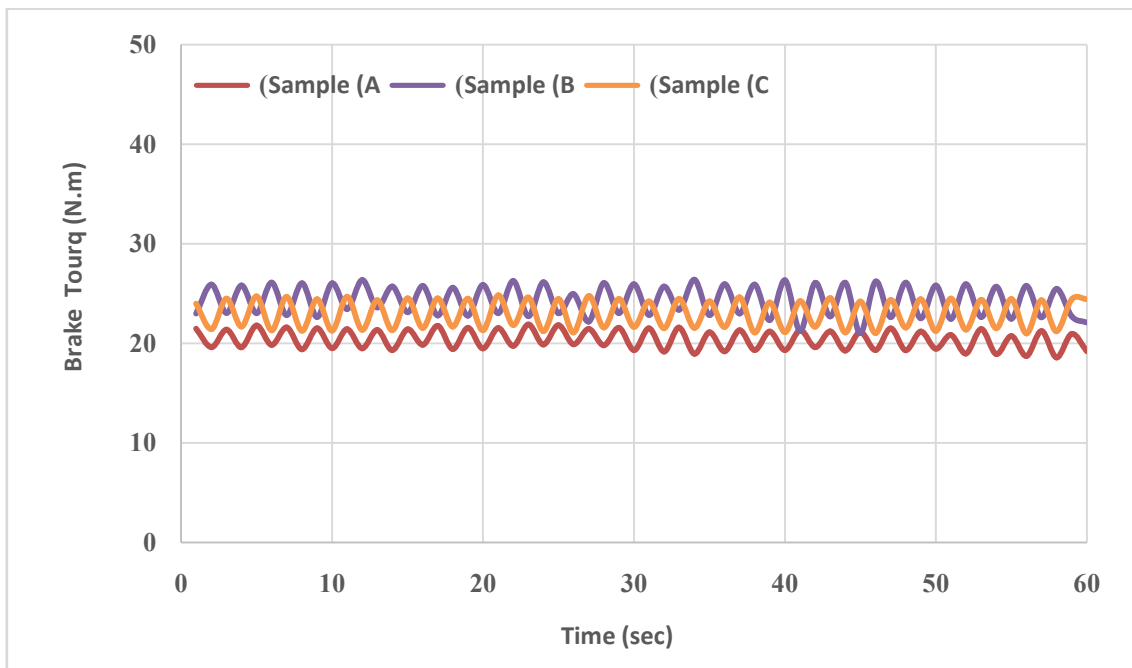


Fig. 11. Effect of alumina on brake tourq of commercial and modified brake pads at sliding speed of 600 rpm at brake oil pressure 2.5 bar

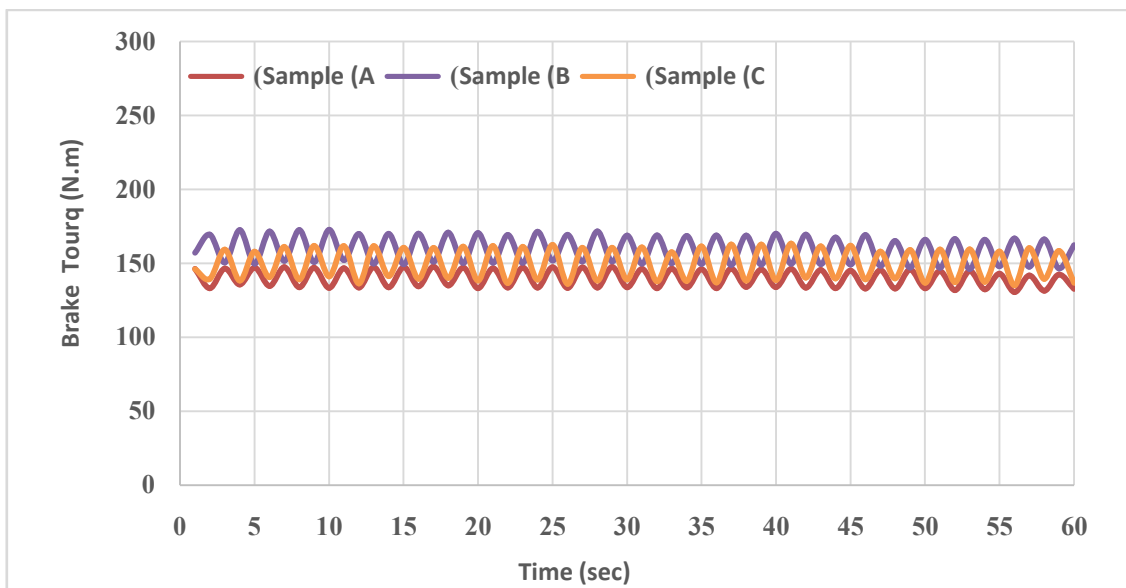


Fig. 12. Effect of alumina on brake torque of commercial and modified brake pads at sliding speed of 600 rpm at brake oil pressure 10 bar

IV. Conclusions

In this study, the average brake force of commercial and modified samples at temperatures of 70 and 130°C at a constant sliding speed of 150 rpm, the average brake force of commercial sample (A) at 70°C is 130.91 and 958.24 N, for modified sample (B) are 148.91 and 1084.59 N, and for modified sample (C) are 140 and 1033.46 N and at an initial temperature of 130°C, the average brake force for commercial sample (A) was 125.83 and 948 N, for modified sample (B) 147 and 1074.37 N, and for modified sample (C) 138.35 and 1014.26 N, respectively at brake oil pressure of 2.5 and 10 bar, the value of mean brake force of sample (B) increases by 12.16%, 11.62% and for sample (c) increases by 7.14%, 7.26% depending on value of mean brake force of commercial sample (A). Also, at a constant sliding speed of 600 rpm at brake oil pressure 2.5 and 10 bar. The results show that the average brake force of commercial sample (A) at 70°C is 114.50 and 784.6718 N, for modified sample (B) are 136.58 and 895.26 N, and for modified sample (C) are 128.70 and 838.42 N, the value of mean brake force of sample (B) increases by 16.17%, 12.40% and for sample (c) increases by 10%, 6.44% depending on value of mean brake force of commercial sample (A). The average friction coefficients for modified samples (B) and (C) are higher than the average friction coefficients for commercial sample (A), because alumina is an abrasive with nanometer diameters that enhances the coefficient of friction. The results showed that the average brake torque of modified samples was higher than the average brake torque of commercial samples with an increase in brake oil pressure from 2.5 to 10 bars and a sliding speed of 600 r.p.m. during a braking time of 60 seconds. This is due to the increase in brake power and friction coefficient under the same operating conditions at each constant speed.

V. Conclusion

A solar desalination system based on free jet-humidification with an auxiliary cold water system was carried out at Suez city, Egypt 29.9668°N, 32.5498°E. The main conclusions items can be briefly systemized as the following:

1. Spherical dome heights 40 cm produce the highest fresh water productivity at the same condition.
2. Increase the condensation surface will be increase the fresh water productivity
3. Increase the salinemass flow rate will be increase the fresh water productivity
4. The system productivity is (2.68 L/m²), the estimated cost is (0.12 \$/L) and the efficiency is 61 %.

References

- [1]. Ajeet B. Bhane, Sandeep M. Salodkar, Hardik B. Ramani (2020). Braking System Approaching towards the Betterment and Its Consequences. International Research Journal on Advanced Science Hub, 2(11), 54-56. <https://doi.org/10.47392/irjash.2020.236>
- [2]. Fauzan Ilham, Maulana, Noorsakti Wahyudi, Indah Puspitasari, (2019). Rancang bangun sistem sistem rem mobil listrik fusena. Jurnal Poli-Teknologi, 18(3), 243-247.
- [3]. Ibrahim L. Ahmed et al, (2020). Study the effect of changing the lining form of the duplex drum brake on the brake performance. International Research Journal of Engineering and Technology (IRJET), 7(7), 1513-1514.

- [4]. Shoab Munir Mulaniet al.,(2022). A review on recent development and challenges in automotive brakepad-disc system. *Jurnal Poli-Teknologi*, 56(1), 2-3. <https://doi.org/10.1016/j.matpr.2022.01.410>
- [5]. Matteo Federici, Stefano Gialanella, Mara Leonardi, Guido Perricone, Giovanni Straffelini,(2018). A preliminary investigation on the use of the pin-on-disc test to simulate off-brake friction and wear characteristics of friction materials. *Jurnal Poli-Teknologi*, 410(411), 1-7. <https://doi.org/10.1016/j.wear.2018.07.011>
- [6]. C Pinca-Bretotean, A L Craciun, C Preda and Arun Kumar Sharma,(2021). Physico-mechanical and tribological characteristics of composites used for brake pads. *Journal of Physics: Conference Series*, 1718(1), 1-6. <https://doi.org/10.1088/1742-6596/1781/1/012032>
- [7]. Giovanna Gautier di Confiengo, Maria Giulia Faga, (2022). Ecological Transition in the Field of Brake Pad Manufacturing: An Overview of the Potential Green Constituents. *Jurnal Poli-Teknologi*, 14(5), 1-7. <https://doi.org/10.3390/su14052508>
- [8]. Zeina Ammar, Hamdy Ibrahim, Mahmoud Adly, Ioannis Sarris and Sherif Mehanny, (2023). Influence of Natural Fiber Content on the Frictional Material of Brake Pads—A Review. *Journal of composites science*, 7(72), 11-12. <https://doi.org/10.3390/jcs7020072>
- [9]. Kumaran Selvaraj et al, (2021). New Developments in Carbon-Based Nanomaterials for Automotive Brake Pad Applications and Future Challenges. *Journal of Nanomaterials*, 2021(3), 1-20. <https://doi.org/10.1155/2021/6787435>
- [10]. Ileana Nicoleta, Lucica Grigora, Ruxandra, (2015). Composite Materials with Complex Compositions used in Vehicle Brake System: a Review. *American Romanian Academy of Arts and Sciences (ARA)*, 58(39), 243-247. <http://dx.doi.org/10.14510/39ARA2015.3913>
- [11]. Mastariyanto Perdana, Meiki Eru Putra, Akmal, Hengki Putra Murfid Ikram, Ardhy Meidianda, (2023). Rancang bangun sistem rem mobil listrik fusena. *JURNAL TEKNIK MESIN INSTITUT TEKNOLOGI PADANG*, 13(1), 12-17. <http://doi.org/10.21063/JTM.2023.v13.i1.13-18>
- [12]. Arpita Chatterjee et al., (2023). Fabrication and Characterization of SiC-reinforced Aluminum Matrix Composite for Brake Pad Applications. *metals*, 13(3), 16. <http://doi.org/10.3390/met13030584>
- [13]. ALCrăciun, C Pinca-Bretotean, C Birtok-Băneasă and A Josan,(2017). Composites materials for friction and braking application. *Journal of IOP Science Materials Science and Engineering*, 200(1), 1-9. <http://doi.org/10.1088/1757-899X/200/1/012009>
- [14]. A LCraciun et al, (2018). Aspects regarding manufacturing technologies of composite materials for brake pad application. *Journal of IOP Science Materials Science and Engineering*, 294(1), 8. <http://doi.org/10.1088/1757-899X/294/1/012003>
- [15]. Vikas Mehta et al., (2023). Comparative Study of Chemically Treated Sugarcane and Kevlar Fiber to Develop Brake Resistance Composites. *MDPI journals*, 28(12), 13. <https://doi.org/10.3390/molecules28124861>
- [16]. Moch. Aziz Kurniawan, Yoga Prasetyo, Srianto, Aat Eska Fahmadi, Rifano, (2022). Characterization of Brake Pads by Variation in Composition of Teak Wood Powder and Rice Husk Ash. *RSF Conference Series: Engineering and Technology*, 2(2), 191. <https://doi.org/10.31098/cset.v2i2.572>
- [17]. J. Abutu et al., (2018). Production and characterization of brake pad developed from coconut shell reinforcement material using central composite design. *Springer Nature Journal Applied Science*, 1(82), 1-7. <https://doi.org/10.1007/s42452-018-0084-x>
- [18]. H Yanar, G Purcek, and H H Ayar, (2020). Effect of steel fiber addition on the mechanical and tribological behavior of the composite brake pad materials. *IOP Conf. Series: Materials Science and Engineering*, 724(1), 1-5. <https://doi.org/10.1088/1757-899X/724/1/012018>
- [19]. Ahmet Keskin, (2011). Investigation of using natural zeolite in brake pad. *Academic Journals*, 6(23), 4894. <https://doi.org/10.5897/SRE10.1072>
- [20]. Worku Mamuye Yilma, Balkeshwar Singh, Getinet Asrat and Nazia Hossain, (2023). Taguchi Method Optimization of Water Absorption Behavior by Wheat Straw-Basalt Hybrid Brake Pad Composite. *Journal of Composites Science*, 7(2), 15. <https://doi.org/10.3390/jcs7020062>
- [21]. Tej Singh et al., (2023). Performance Optimization of Lignocellulosic Fiber-Reinforced Brake Friction Composite Materials Using an Integrated CRITIC-CODAS-Based Decision-Making Approach. *MDPI journals*, 15(11), 15-16. <https://doi.org/10.3390/su15118880>
- [22]. Benedict U. Iyida, Azubuike M. Nwankwo, Thomas O. Onah, (2023). Parametric Effects on the Coefficient of Friction of a Novel Composite Material for Automobile Brake Lining. *INTERNATIONAL RESEARCH JOURNAL OF MULTIDISCIPLINARY TECHNOVATION*, 5(4), 12. <https://doi.org/10.54392/irjmt2342>
- [23]. Khaled Abdelwahed et al., (2019). Effect of the sliding speed on the performance of conventional and modified disc brakes at different initial operating temperatures. *International Journal of Engineering Inventions*, 7(10), 46-61.
- [24]. Rewida Sami Abdullah et al., (2022). Effect of Sliding Speed on the Performance of Coated Ventilated Disc Brake. *International Journal of Engineering Inventions*, 4(9), 1350-1357. <https://doi.org/10.35629/5252-040913501358>
- [25]. Siti Shofiah, (2025). Statistical Analysis of Temperature Effects on Brake Force and Efficiency in Vehicle Braking Systems: A Comprehensive Study. *E3S Web of Conferences*, 622 (01003), 2-6. <https://doi.org/10.1051/e3sconf/202562201003>

References

- [1]. Patel, H., Patel, P. and Patel, J. [2012] "Review of solar distillation methods" *International Journal of Advanced Engineering Research and Studies*, Vol. II, Issue I: pp.157–161.
- [2]. Shatat, M., Worall, M. and Riffat, S. [2013] "Opportunities for solar water desalination worldwide: Review" *Sustainable Cities and Society*, Vol. 9: pp.67–80.
- [3]. Sivakumar, V. and Sundaram, E. G. [2013] "Improvement techniques of solar still efficiency: A review" *Renewable and Sustainable Energy Reviews*, Vol. 28: pp.246–264.
- [4]. Sharon, H. and Reddy, K. S. [2015] "A review of solar energy driven desalination technologies" *Renewable and Sustainable Energy Reviews*, Vol. 41: pp.1080–1118.
- [5]. Franchini, G. and Perdichizzi, A. [2014] "Modeling of a solar driven HD (Humidification-Dehumidification) desalination system" *Energy Procedia*, Vol. 45: pp.588–597.
- [6]. Zamen, M., Soufari, S. M., AbbasianVahdat, S., Amidpour, M., Zeinali, M. A., Izanloo, H. and Aghababaie, H. [2014] "Experimental investigation of a two-stage solar humidification–dehumidification desalination process" *Desalination*, Vol. 332: pp.1–6.

- [7]. Ghalavand, Y., Hatamipour, M. S. and Rahimi, A. [2014] "Humidification compression desalination" *Desalination*, Vol. 341: pp.120–125.
- [8]. Kabeel, A. E. and El-said, E. M. S. [2014] "A hybrid solar desalination system of air humidification, dehumidification and water flashing evaporation: II. Experimental investigation" *Desalination*, Vol. 341: pp.50–60.
- [9]. Li, X., Yuan, G., Wang, Z., Li, H. and Xu, Z. [2014] "Experimental study on a humidification and dehumidification desalination system of solar air heater with evacuated tubes" *Desalination*, Vol. 351: pp.1–8.
- [10]. Yildirm, C. and Solmus, I. [2014] "A parametric study on a humidification–dehumidification (HDH) desalination unit powered by solar air and water heaters" *Energy Conversion and Management*, Vol. 86: pp.568–575.
- [11]. Nada, S. A., Elattar, H. F. and Fouda, A. [2015] "Experimental study for hybrid humidification–dehumidification water desalination and air conditioning system" *Desalination*, Vol. 363: pp.112–125.
- [12]. Elminshawy, N. A. S., Siddiqui, F. R. and Addas, M. F. [2015] "Experimental and analytical study on productivity augmentation of a novel solar humidification–dehumidification (HDH) system" *Desalination*, Vol. 365: pp.36–45.
- [13]. Muthusamy, C. and Srithar, K. [2015] "Energy and exergy analysis for a humidification–dehumidification desalination system integrated with multiple inserts" *Desalination*, Vol. 367: pp.49–59.
- [14]. He, W. F., Han, D., Xu, L. N., Yue, C. and Pu, W. H. [2016] "Performance investigation of a novel water–power cogeneration plant (WPCP) based on humidification dehumidification (HDH) method" *Energy Conversion and Management*, Vol. 110: pp.184–191.
- [15]. Wu, G., Zheng, H., Kang, H., Yang, Y., Cheng, P. and Chang, Z. [2016] "Experimental investigation of a multi-effect isothermal heat with tandem solar desalination system based on humidification–dehumidification processes" *Desalination*, Vol. 378: pp.100–107.
- [16]. Giwa, A., Akther, N., AlHousani, A., Haris, S. and Hasan, S. W. [2016] "Recent advances in humidification dehumidification (HDH) desalination processes: Improved designs and productivity" *Renewable and Sustainable Energy Reviews*, Vol. 57: pp.929–944.
- [17]. Giwa, A., Fath, H. and Hasan, S. W. [2016] "Humidification–dehumidification desalination process driven by photovoltaic thermal energy recovery (PV-HDH) for small-scale sustainable water and power production" *Desalination*, Vol. 377: pp.163–171.
- [18]. Sharshir, S. W., Peng, G., Yang, N., El-Samadony, M. O. A. and Kabeel, A. E. [2016] "A continuous desalination system using humidification – dehumidification and a solar still with an evacuated solar water heater" *Applied Thermal Engineering*, Vol. 104: pp.734–742.
- [19]. Behnam, P. and Shafii, M. B. [2016] "Examination of a solar desalination system equipped with an air bubble column humidifier, evacuated tube collectors and thermo syphon heat pipes" *Desalination*, Vol. 397: pp. 30–37.
- [20]. Eldesouki I., Reda A., Mohamed A. [2018] "An experimental study of solar desalination using free jets and an auxiliary hot air stream" *Heat Mass Transfer*, Vol. 54: Issue 4, pp. 1177–1187.
- [21]. Arunkumar, T., Jayaprakash, R., Denkenberger, D., Ahsan, A., Okundamiya, M. S., kumar, S., Tanaka, H. and Aybar, H. S. [2012] "An experimental study on a hemispherical solar still" *Desalination*, Vol. 286: pp.342–348.
- [22]. Arunkumar, T., Vinothkumar, K., Ahsan, A., Jayaprakash, R. and Kumar, S. [2012] "Experimental Study on Various Solar Still Designs" *International Scholarly Research Network ISRN Renewable Energy*, Vol. 2012: Article ID 569381, 10 pages.
- [23]. Panchal, H. N., Prajapati, V., Goswami, R. and Pancholi, N. [2012] "Performance analysis of hemispherical solar still in climate condition of Mehsana, Gujarat" *International Journal of Advanced Engineering Research and Studies*, Vol. I, Issue III: pp.210–213.
- [24]. Solanki, A. S., Soni, U. R. and Patel, P. [2014] "Comparative Study on Hemispherical Solar Still with Black Ink Added" *International Journal of Engineering Research and General Science*, Vol. 2, Issue 3: pp.2091–2730.
- [25]. Tabrizi FF, Khosravi M, Sani IS [2016] "Experimental study of a cascade solar still coupled with a humidification–dehumidification system" *Energy Convers Manag*, Vol. 115: pp.80–88.
- [26]. Deniz E, Cinar S [2016] Energy, exergy, economic and environmental (4E) analysis of a solar desalination system with humidification-dehumidification energy. *Convers Manag*, Vol.126: pp.12–19.